Cell, Vol. 72, 779–790, March 12, 1993, Copyright ©1993 by Cell Press

Binding of a High Affinity Phosphotyrosyl Peptide to the Src SH2 Domain: Crystal Structures of the Complexed and Peptide-free Forms

Gabriel Waksman,* Steven E. Shoelson,‡ Nalin Pant,* David Cowburn,* and John Kuriyan*†
*The Rockefeller University
†Howard Hughes Medical Institute
New York, New York 10021
‡Joslin Diabetes Center and Department of Medicine
Brigham and Women's Hospital
Harvard Medical School
Boston, Massachusetts 02215

Summary

The crystal structure of the Src SH2 domain complexed with a high affinity 11-residue phosphopeptide has been determined at 2.7 Å resolution by X-ray diffraction. The peptide binds in an extended conformation and makes primary interactions with the SH2 domain at six central residues: PQ(pY)EEI. The phosphotyrosine and the isoleucine are tightly bound by two well-defined pockets on the protein surface, resulting in a complex that resembles a two-pronged plug engaging a two-holed socket. The glutamate residues are in solvent-exposed environments in the vicinity of basic side chains of the SH2 domain, and the two N-terminal residues cap the phosphotyrosine-binding site. The crystal structure of Src SH2 in the absence of peptide has been determined at 2.5 Å resolution, and comparison with the structure of the high affinity complex reveals only localized and relatively small changes.

Introduction

Src homology 2 (SH2) domains were first identified from sequence similarities in the noncatalytic regions of Src-related tyrosine kinases, spanning approximately 100 amino acid residues (Sadowski et al., 1986). The subsequent discovery that SH2 domains bind to specific phosphorylated tyrosine residues has provided a link between tyrosine kinases and proteins that respond to tyrosine phosphorylation (for reviews see Koch et al., 1991; Pawson and Gish, 1992; Mayer and Baltimore, 1993). The transmission of growth factor–mediated signals, for example, depends critically on the the sequence-specific recognition of phosphorylated tyrosines by SH2 domains, which have been discovered in a number of proteins that act downstream of growth factor receptors, including Ras GTPase-activating protein (GAP), phosphatidylinositol 3′-kinase (PIK), and phospholipase C-γ (reviewed by Cantley et al., 1991). SH2 domains serve to localize these proteins to activated receptors and are implicated in the modulation of enzymatic activity (O'Brien et al., 1990; Roussel et al., 1991; Backer et al., 1992).

While SH2 domains share the common property of binding phosphotyrosine-containing peptides, additional biological specificity resides in the sequence contexts of the phosphotyrosine. This has been demonstrated clearly by the differential binding of the SH2 domains of proteins such as the p85 subunit of PIK, Ras GAP, and phospholipase C-γ to activated growth factor receptors (Moran et al., 1990; Birge et al., 1992; Fantl et al., 1992; Kashishian et al., 1992; Klippel et al., 1992; Rotin et al., 1992; Escobedo et al., 1991). The general architecture of SH2 domains and the mechanism of phosphotyrosine recognition have been clarified by crystal structures of Src SH2 domain complexed with low affinity phosphopeptides (Waksman et al., 1992) and by nuclear magnetic resonance solution structures of the uncomplexed forms of the SH2 domains of the Abl tyrosine kinase (Overduin et al., 1992b) and the p85 subunit of PI 3′-OH kinase (Booker et al., 1992). The two peptides used in the previous crystallographic work bound Src SH2 rather weakly, with millimolar concentrations of peptide being required to compete for SH2 binding with phosphorylated epidermal growth factor receptor (Waksman et al., 1992). Thus, although highly specific interactions were observed between the SH2 domain and the phosphotyrosine side chain, almost no interactions were seen between the rest of the peptide and the protein. This prevented the definition of the recognition sites for the flanking sequences, and the mechanism of sequence specificity remained an open question.

From peptide competition and receptor mutagenesis experiments on the receptors for platelet-derived and epidermal growth factors and the SH2 domains of p85, phospholipase C-γ, and GAP (Fantl et al., 1992; Kashishian et al., 1992; Rotin et al., 1992), it appears that short peptide sequences suffice to capture the essential elements of sequence-specific recognition. For example, the two SH2 domains of p85α bind to sequences in the platelet-derived growth factor receptor that contain methionine or valine at the first position following the phosphotyrosine, and methionine at the third position. In contrast, GAP binds most efficiently to a site in the platelet-derived growth factor receptor that contains methionine at the first position, with proline and tyrosine at the third and fourth positions, respectively (Fantl et al., 1992; Kashishian et al., 1992).

The general question of sequence specificity in phosphopeptide–SH2 interactions has been addressed recently by Cantley and coworkers, who used a screening method to select phosphopeptides that bind to any particular SH2 domain, starting from a mixture of peptides that are degenerate at the three positions following the phosphotyrosine (Songyang et al., 1993 [this issue of *Cell*]). This led to the identification of the motif pYEEI (more generally, two nonbasic polar residues following the phosphotyrosine and a large hydrophobic residue at the fourth position) as being optimal for binding to Src SH2. An 11-residue phosphotyrosyl peptide corresponding to a sequence found in hamster middle T antigen (EPQ**pYEEI**-PIYL) contains this motif and has been shown to bind Src SH2 with high affinity (estimated K_D = 3–6 nM) (Payne et al., submitted; Songyang et al., 1993). We refer to this peptide as YEEI. Previously, reported peptide binding

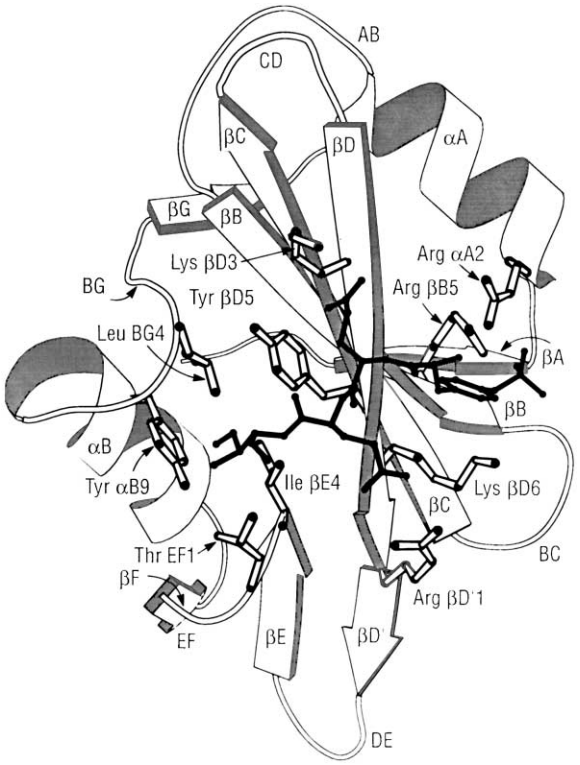

Figure 1. Schematic Diagram of the Src SH2 Domain, Illustrating the Notation Used

The phosphotyrosine (at the right), Glu(+1), Glu(+2), and Ile(+3) (at the left) of the peptide are shown with solid black bonds and are not labeled explicitly, α helices and β strands are shown as ribbons and arrows, respectively. Several of the side chains involved in peptide binding are shown as stick figures and are labeled according to the secondary structure notation used in this paper (see Figure 2).

studies on Src SH2 involved the tyrosine-phosphorylated C-terminal tail of c-Src, which was shown to be involved in suppressing kinase activity by interacting with the SH2 domain (Roussel et al., 1991). The YEEI peptide binds to Src SH2 with ~100-fold higher affinity than a peptide corresponding to the C-terminal region of Src (Payne et al., submitted) and is more efficient at activating c-Src (Liu et al., 1993).

We present the crystal structure, determined at a resolution of 2.7 Å, of the complex of Src SH2 domain with the 11-residue YEEI peptide. In addition, we have determined the structure of the uncomplexed form of Src SH2, at a resolution of 2.5 Å. We show that the high affinity SH2–peptide complex resembles a two-holed socket (the SH2 domain) engaging a two-pronged plug (the phosphopeptide). The two holes of the socket correspond to highly specific interaction sites on the surface of SH2. One site, identified previously in the low affinity complexes (Waksman et al., 1992), binds the phosphotyrosine with ion-pairing, hydrogen-bonding, amino-aromatic, and hydrophobic interactions. The second site is mainly hydrophobic in character and serves to bind the isoleucine of the YEEI motif. To interact at both binding sites, the peptide adopts an extended conformation and spans the surface of the SH2 domain within 4 residues. Comparison with the structure of the uncomplexed form of Src SH2 reveals that highly localized and relatively small conformational changes occur upon peptide binding. These changes represent an induced-fit response in the protein, whereby the highly charged phosphate-binding pocket opens up and becomes solvent exposed in the absence of peptide, and the hydrophobic pocket closes up slightly. No significant change in structure is observed anywhere else in the domain.

The relatively high level of sequence conservation observed for SH2 domains makes the results described here of general significance. The phosphotyrosine- and hydrophobic-binding sites are conserved in SH2 domains. Given the small size of the binding surface, these two pockets serve to define a common orientation for bound peptides, simplifying the analysis of the determinants of specificity.

Results

The three-dimensional structures of p85, Abl, and Src SH2 domains are strikingly similar and share a common secondary structure framework and considerable similarity in tertiary fold (Booker et al., 1992; Overduin et al., 1992b; Waksman et al., 1992). To simplify discussion of SH2 structure while emphasizing this common scaffolding, we adopt the notation used by Harrison and coworkers in their discussion of Lck SH2 structure (Eck et al., submitted). The two α helices are denoted αA and αB, and the β strands are labeled βA through βG. Loops connecting secondary structural elements are then denoted uniquely by the alphabetical labels of the adjacent helices or strands: AA, AB, BC, and so on (Figure 1). Each amino acid residue is denoted by its relative position in a secondary structural element, defined using the alignment suggested by Eck et al. (submitted) (Figure 2). Thus, the strictly conserved arginine that coordinates the phosphate group is referred to as Arg βB5 and the highly conserved tryptophan is Trp βA1. A schematic representation of Src SH2 structure is shown in Figure 1, with the elements of secondary structure and important residues labeled according to this nomenclature. Peptide residues of YEEI are numbered relative to the phosphotyrosine: Glu(−3), Pro(−2), Gln(−1), pTyr(0), Glu(+1), Glu(+2), Ile(+3), Pro(+4), Ile(+5), Tyr (+6), Leu(+7).

Crystals of the complexed and uncomplexed forms of Src SH2 have more than one molecule in the crystallographic asymmetric unit. Several independent views of the SH2 domain are thus obtained in each case: three of the high affinity complex (designated Mol1, Mol2, and Mol3) and four of the unliganded protein (designated MolA to MolD). One advantage of this is that the effects of crystal packing interactions can be accounted for, since they are different for each particular molecule. Also, despite the medium resolution of the X-ray analysis, the details of the atomic interactions presented here are relatively reliable because they are observed in three or four crystallographically independent molecules.

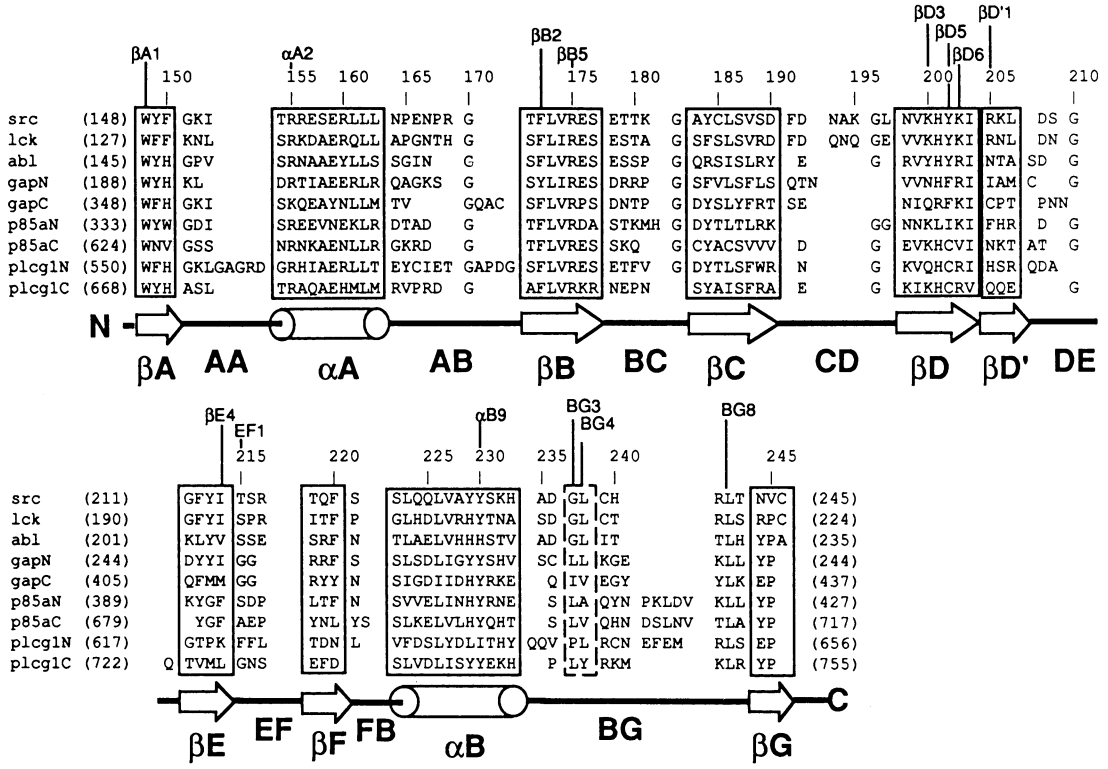

Figure 2. Alignment of SH2 Sequences and Definition of the Residue Notation

The sequences of SH2 domains from Src, Lck, Abl, GAP, the p85 subunit of PIK, and phospholipase C-γ are aligned, based on the secondary structure definitions used in the paper. The two α helices are extended to include N-cap residues. The boundaries of the secondary structural elements are shown by solid boxes, and the notation for these elements is shown schematically at the bottom. The starting residue numbers from the parent sequences are shown on the left, and the v-Src residue numbers are shown above the Src sequence. The new notation is used to identify key functional residues, and these are indicated by dark vertical lines. The 2 residues in the broken box play key roles in mediating peptide binding at the +3 site (see text).

Overall Structure

The spine of the SH2 domain is an uninterrupted β meander, which runs from βB to βF and forms two distinct β sheets. The two sheets are connected by a single continuous β strand, denoted βD in the first sheet and βD′ in the second. The central β sheet (strands B, C, and D) is at the core of the structure and divides the domain into two functionally distinct sides. One side, containing helix αA and one face of the central sheet, is concerned primarily with binding the phosphotyrosine. The other side provides binding sites for the three peptide residues immediately following the phosphotyrosine, and contains helix αB, the smaller β sheet (D′, E, and F), a long loop (BG), and the other face of the central sheet. The backbone of the peptide runs along a surface that is perpendicular to the central β sheet (Figure 1). The N- and C-termini of the SH2 domain are located opposite to this peptide-binding surface, near strand B of the central β sheet, with the polypeptide chain entering and leaving the domain at short strands (βA and βG) that hydrogen bond with βB. These two short strands serve to cap the hydrophobic core of the domain.

Peptide Binding Interactions

The 11-residue YEEI peptide binds in an extended conformation and makes contacts with the SH2 domain primarily at four residues: the phosphotyrosine, Glu(+1), Glu(+2), and Ile(+3). In addition, the polypeptide backbone at −1 and the proline ring at −2 are involved in capping the phosphotyrosine-binding site. Strong electron density is observed for residues −2 to +3 in all three SH2 molecules in the asymmetric unit of the crystal, except for the side chain of Gln(−1) (Figure 3). Peptide residues outside this central region are partially or completely disordered, except in Mol3 where electron density is clearly visible for 10 of the 11 residues. This is due to residues +5 to +7 of the Mol3 peptide being sandwiched between two neighboring SH2 molecules in the crystal lattice. In no case does an adjacent molecule in the crystal lattice interact closely with peptide atoms at the phosphotyrosine, +1, +2, or +3 site. The conformation of the peptide is very similar in all three crystallographically independent molecules. When the three SH2 domains are superimposed, the root mean square (RMS) deviation in atomic positions for the phosphotyrosine and the following 3 residues of the peptide is 0.33 Å for C^{α} atoms and 0.72 Å for all atoms. The three SH2 molecules in the asymmetric unit also show no significant structural deviations (RMS deviation in atomic positions is 0.39 Å for C^{α} atoms and 0.97 Å for all atoms in helices and strands).

The YEEI peptide fits snugly onto the surface of the SH2

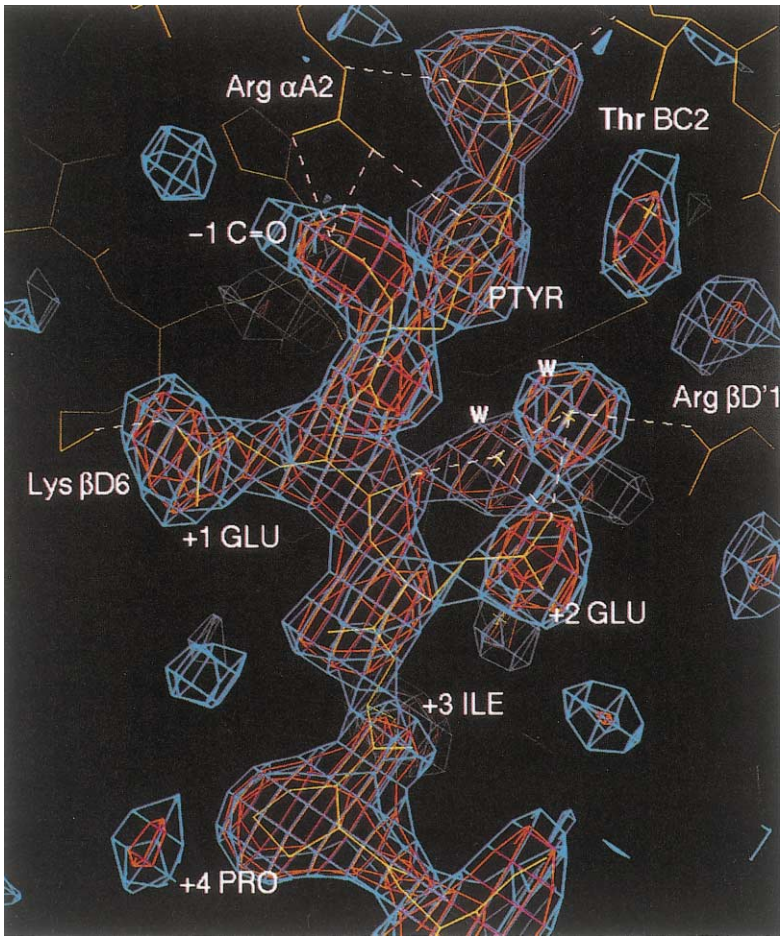

Figure 3. Electron Density for the YEEI Peptide at 2.7 Å Resolution, Shown in a Chicken Wire Representation

The protein and peptide atoms are shown in yellow. Hydrogen-bonding interactions are indicated by dotted lines. Blue contour lines indicate electron density at 0.8 σ, and red at 1.5 σ above the mean density, in a map calculated using coefficients $(|F_o| - |F_c|)\exp(-i\alpha_c)$, where $|F_c|$ is the observed structure factor amplitude, and $|F_o|$ and α_c are the amplitudes and phases calculated from a model that does not include the peptide.

domain, in contrast with the low affinity peptide structures described previously, in which the peptides make significant contacts with the SH2 domain at the phosphotyrosine-binding site alone (Waksman et al., 1992). The most striking structural difference between the low and high affinity complexes is that in the latter the isoleucine residue at +3 is bound tightly by a number of hydrophobic residues. A cross section of the SH2-peptide complex is shown in Figure 4A, and it can be seen that the peptide inserts the side chains of the phosphotyrosine and Ile(+3) into two pockets in the SH2 domain. These pockets are at opposite edges of the binding surface, and the peptide backbone is directed away from the SH2 domain before the phosphotyrosine and after the isoleucine. The two glutamate side chains in the middle lie along the surface and make weak polar interactions with neighboring residues (see below).

The docking of the phosphotyrosine and the isoleucine (the two prongs) results in an extensive interaction surface between the peptide and the protein, with approximately half of the peptide surface inaccessible to solvent in the complex. The surface areas that are occluded on complex formation are 410 and 600 Å^2, for the SH2 domain and the peptide, respectively (these are the differences in solvent-accessible area [Richards, 1977] for the complexed and isolated molecules, calculated using a probe of radius 1.4 Å). A survey of protein–protein recognition surfaces shows that the buried surface areas of the partners in tight complexes range from 650 to 1000 Å^2 (Janin and Chothia, 1990). In the cases surveyed both partners in the interactions are folded proteins, and it is remarkable that the interaction of the SH2 domain with the relatively short YEEI peptide achieves almost comparable surface burial.

The two-pronged socket nature of the SH2–peptide interaction is further demonstrated in Figure 4B, which shows the solvent-accessible surface (Richards, 1977) of the SH2 domain, for the YEEI complex structure with the peptide removed. The surface is colored based on the local electrostatic potential, calculated using the GRASP program of Nicholls and Honig, with arginines and lysines treated as positively charged, glutamates and aspartates as negatively charged, and all other residues (including histidines) as neutral (Gilson et al., 1988; Nicholls et al., 1991). Regions of positive and negative electrostatic potential are colored blue and red, respectively, while neutral regions are white. Two well-defined pockets in the surface are strikingly evident. One is a region of positive electrostatic potential and corresponds to the phosphotyrosine-binding site. The other pocket is neutral in charge and is lined by hydrophobic residues and serves to bind the isoleucine. The glutamates at positions +1 and +2 appear

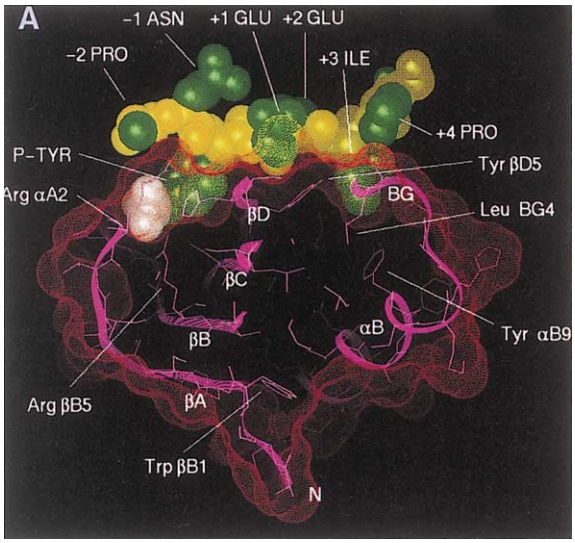

Figure 4. Molecular Surfaces of the SH2 Domain

(A) A cutaway view of the SH2 domain, showing the interactions with YEEI peptide. The accessible surface area (Richards, 1977) is represented by red dots, and the polypeptide backbone of SH2 is shown as a purple ribbon. Protein atoms are shown as purple bonds. The peptide is shown as a space-filling model, with side chains colored green and the backbone yellow. The phosphate group is shown in white. Note that some atoms of the proline ring (−1) are obscured in this cross section.

(B) The molecular surface of the YEEI complex (Richards, 1977), calculated and displayed using GRASP (Nicholls et al., 1991) for Mol1 with the peptide removed. The surface is colored according to the local electrostatic potential and is colored deep blue in the most positive regions and deep red in the most negative, with linear interpolation for values in between. The two binding pockets on the surface are outlined in yellow, and important residues are identified by red arrows. This view of the SH2 domain is very similar to that seen in Figures 1 and 5A.

(C) The molecular surface of the uncomplexed form of Src SH2, displayed as in (B), for MolD.

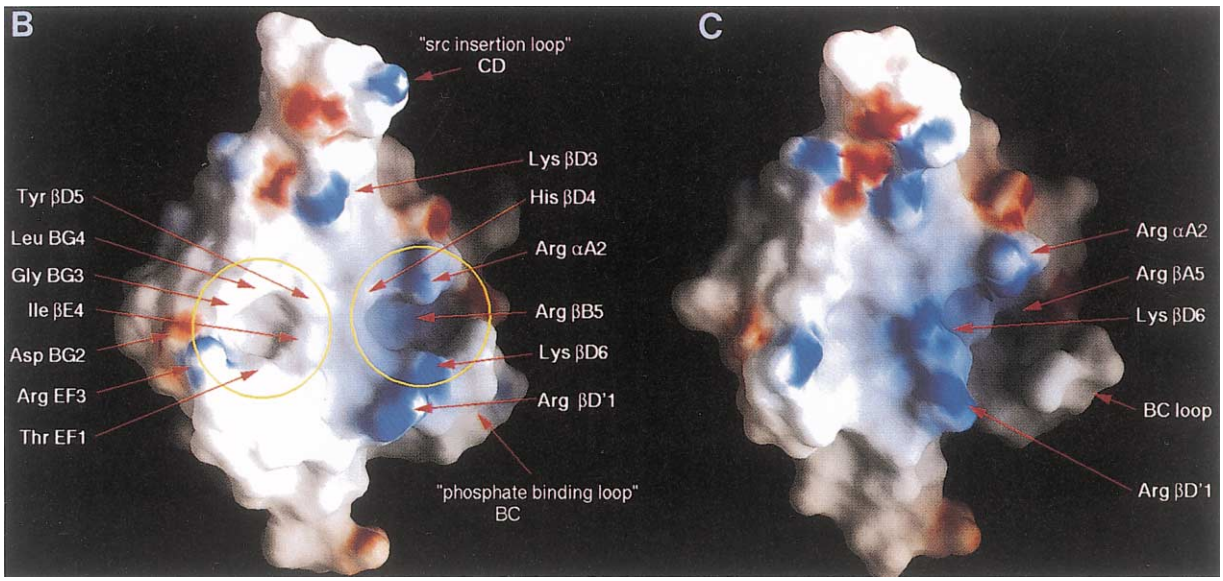

to be stabilized by two regions of positive electrostatic potential due to Lys βD3 (at +1) and Arg βD′1 (at +2).

A shallow groove on the surface of the protein, between Lys βD3 and His βD4 in Figure 4B, had previously been indentified as a potential binding site for peptide residues N-terminal to the phosphotyrosine. A prominent feature at one edge of this groove is the large projection formed by the CD loop, the site of a 4-residue insertion specific to Src family SH2 domains (Figure 4B). This region does not interact directly with the YEEI peptide, but its disposition suggests potential interactions with longer peptides or with other regions of intact Src. In the YEEI peptide, the proline at position −2 caps the phosphotyrosine-binding site (Figure 4A) and is positioned between Arg αA2 and Thr BC2. The glutamate at −3 is disordered in all three molecules.

Phosphotyrosine Interactions

The previous X-ray analysis on low affinity peptide complexes of Src SH2 was done at high resolution (1.5 Å), and the interactions that stabilize the phosphotyrosine were characterized quite precisely (Waksman et al., 1992). The resolution of the present work (2.7 Å) does not allow for completely unambiguous definition of hydrogen-bonding interactions, but we take advantage of the presence of three independent molecules in the crystal and present interatomic distances that are averages over the three structures (see schematic diagram in Figure 6A). These confirm that the mode of phosphotyrosine binding is almost exactly the same as in the low affinity complexes, with one important difference. The peptides used in the previous work had N-terminal phosphotyrosines, which resulted in the terminal amino groups forming unfavorable

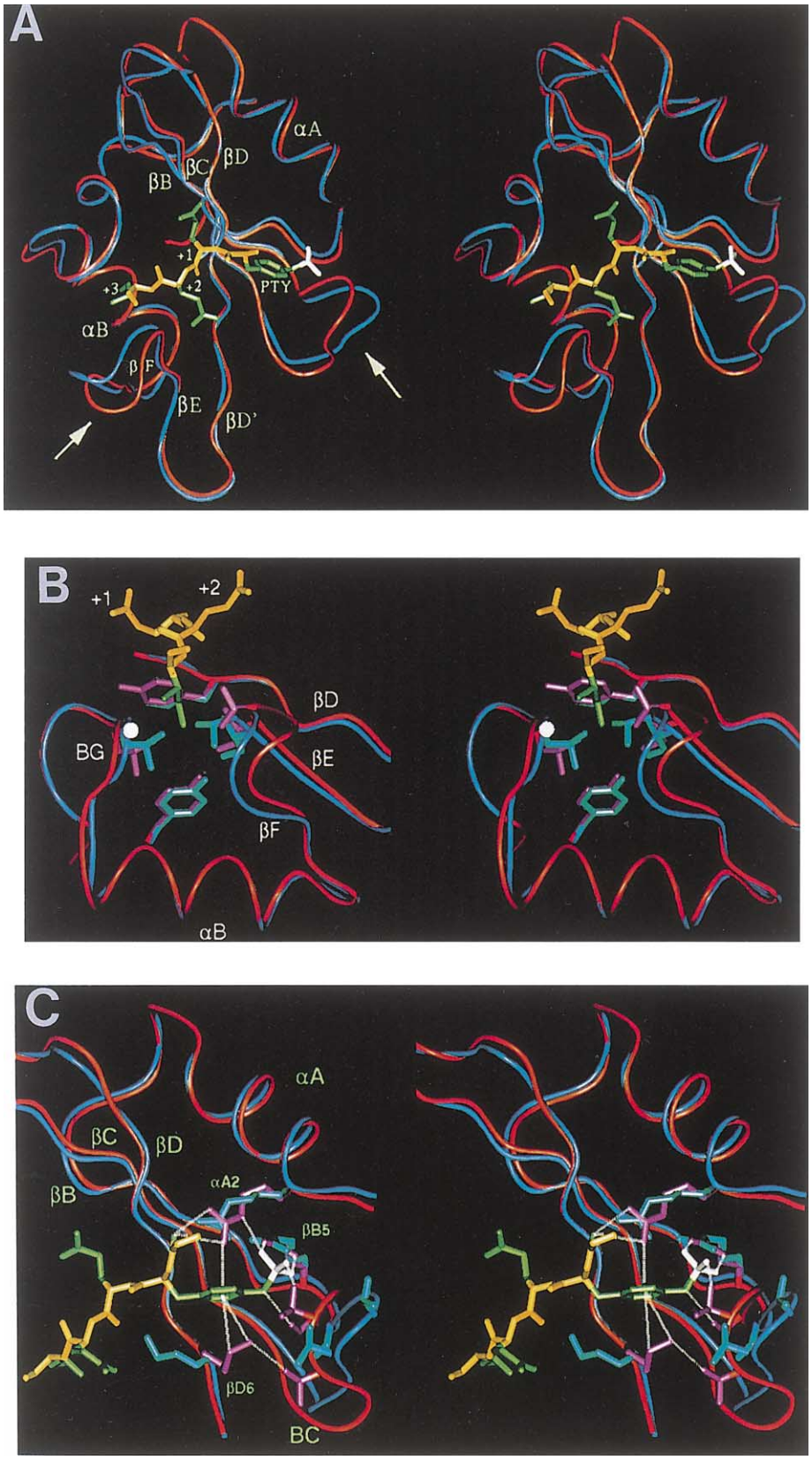

Figure 5. Comparison of Complexed and Uncomplexed SH2 Structures

(A) Stereodiagram of the SH2 domain, showing the regions of peptide-induced conformational changes. The polypeptide backbone of the YEEI complex is shown as a red tube, and that of the uncomplexed form is shown in blue. The peptide (residues 0 to +3) is shown in green and yellow.

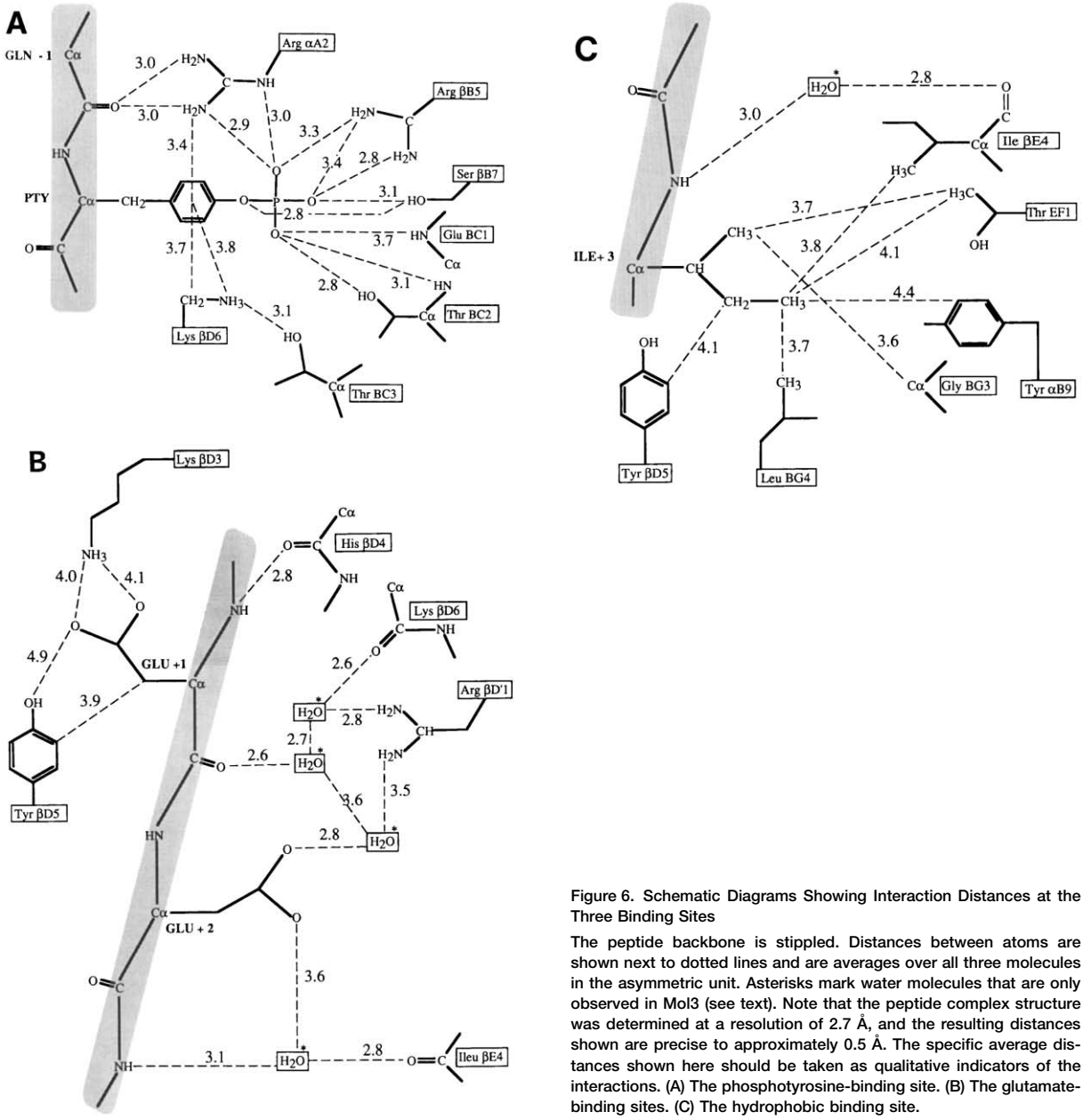

Figure 6. Schematic Diagrams Showing Interaction Distances at the Three Binding Sites

The peptide backbone is stippled. Distances between atoms are shown next to dotted lines and are averages over all three molecules in the asymmetric unit. Asterisks mark water molecules that are only observed in Mol3 (see text). Note that the peptide complex structure was determined at a resolution of 2.7 Å, and the resulting distances shown are precise to approximately 0.5 Å. The specific average distances shown here should be taken as qualitative indicators of the interactions. (A) The phosphotyrosine-binding site. (B) The glutamate-binding sites. (C) The hydrophobic binding site.

interactions with Arg αA2. In the case of the YEEI peptide, the carbonyl group of the residue at −1 forms hydrogen-bonding interactions with the terminal nitrogens of Arg αA2. Another distinctive feature of the N-terminal extension is that the proline ring at position −2 stacks over the phosphotyrosine and shields the phosphate group and the edge of the tyrosine ring from solvent.

The important elements of phosphotyrosine recognition are provided by αA, βB, βD, and the loop connecting strands B and C (Figure 5B). In the peptide complexes, the BC loop closes over the phosphate and, together with the side chains of Lys βD6, His βD4, and Arg αA2, forms the mouth of the phosphotyrosine-binding site. Arg βB5, which is strictly conserved, is at the base of this pocket and is involved in a bidentate ion pairing interaction with the phosphate group. Lys βD6 and His βD4 both provide

(B) Close-up of the hydrophobic binding site, in stereo, with selected side chains. The YEEI complex is shown in red, with pink side chains, and the uncomplexed form is shown in blue, with gray side chains. (C) As in (B), for the phosphotyrosine-binding site. Hydrogen-bonding interactions in the complexed form are shown as dotted lines. Gly BG3 is indicated by a white dot.

hydrophobic interactions with the ring system. Lys βD6 and Arg αA2 form amino-aromatic interactions with the ring of the phosphotyrosine. In addition, Lys βD6 is hydrogen bonded to Thr BC3 in the phosphate-binding loop, and Arg αA2 donates hydrogen bonds to a phosphate oxygen as well as to the peptide bond at position −1.

The Hydrophobic Binding Pocket

The isoleucine side chain at +3 is almost completely buried at the hydrophobic binding site, as demonstrated by accessible surface area calculations for the isolated peptide and the peptide–SH2 complex, which show that the pocket protects 95% of the side chain surface area from exposure to solvent. The binding pocket is formed by two loops (EF and BG) that frame the C-terminal helix and jut out to form jaws that engulf the peptide side chain (Figure 5C). The base of the binding pocket is formed by helix αB, while the edges are lined by residues provided by the two loops as well as βD (see schematic in Figure 6C). The resulting binding site is critical for determining peptide specificity, as it serves to anchor and orient the peptide on the surface of the SH2 domain. The general hydrophobic character of the pocket is conserved in SH2 domains (see Figure 2), but the variable nature of the specific groups that form the pocket allows for specificity at this site. For example, as discussed later, the backbone C^{α} atom of Gly BG3 makes a close contact with the β branch of the Ile(+3) side chain. Substitution of glycine at this position is likely to destabilize isoleucine binding, and may explain the preference for methionine that is seen in p85, where this residue is a leucine.

The Glutamate-Binding Sites

In contrast with the phosphotyrosine and isoleucine sites, no binding pockets are present for the glutamate residues at positions +1 and +2. Both side chains lie along the surface of the SH2 domain and are almost completely accessible to solvent. In all three molecules the carboxyl group of Glu(+1) interacts with the amino group of Lys βD3 (see Figures 1 and 6B). The nitrogen–oxygen distances are around 4 Å, indicating a somewhat weak ionic hydrogen bond. Although lysine side chains on protein surfaces are often disordered, Lys βD3 is held in place by a strong hydrogen bond with Asn βD1, an interaction that is preserved in the low affinity complex and the uncomplexed form. The C^{β} atom of Glu(+1) also makes a hydrophobic contact with the ring of Tyr βD5, but the carboxyl group is too far away from the tyrosine hydroxyl for hydrogen-bonding interactions.

Glu(+2) makes no direct or water-mediated contacts with the SH2 domain in Mol1 and Mol2. However, in Mol3 three well-resolved water molecules form a hydrogen-bonding network that links Glu(+2) with Arg βD′1, Lys βD6, and the carbonyl oxygen of Glu(+1) (see Figures 3 and 6B). The peptide bound to Mol3 is the best resolved as it is held down by crystal packing interaction at positions +5 to +7, and the increased stability may serve to localize these water molecules. That these interactions are seen in only 1 of the 3 molecules emphasizes that they are not particularly strong and that the selection of glutamate at this position is primarily due to negative factors. This portion of the peptide is completely exposed to solvent, which would disfavor hydrophobic residues. Although the interaction with Arg βD′1 and Lys βD6 is not a strong one, these residues serve to set up a local region of positive charge, and basic residues at position +2 would be disfavored.

Structural Differences between the Complexed and Uncomplexed Forms

Two of the four independent molecules of the uncomplexed form (MolA and MolB) are essentially identical in structure to the YEEI complex (see below). The other two (MolC and MolD) differ from the complexed structure at the phosphotyrosine and hydrophobic binding sites (Figure 5A). Although the structural core of the SH2 domain is preserved, with RMS deviation in C^{α} positions of 0.5 Å between Mol1 (complexed) and MolD (uncomplexed) in strands and helices, the structure changes slightly but significantly in the BC and EF loop regions. At the phosphotyrosine-binding site, the BC loop moves away and becomes relatively disordered, resulting in a more open binding site that exposes Arg βB5 to solvent. Specifically, the C^{α} positions of Glu BC1, Thr BC2, and Thr BC3 shift by 1.9, 3.8, and 1.7 Å, respectively, with respect to the complexed structure. The effect at the isoleucine-binding site is in the opposite direction, in that the uncomplexed structure is more closed than the YEEI complex. The largest shifts are seen at Thr EF1, Ser EF2, and Arg EF3 (1.3, 2.6, and 2.3 Å, respectively). The molecular surface of MolD is shown in Figure 4C, and it can be seen that the phosphotyrosine- and isoleucine-binding pockets are distorted.

These structural changes are not evident in MolA or MolB. A tightly bound phosphate ion is found at the phosphotyrosine-binding site of MolA (data not shown). This ion is bound almost precisely at the site occupied by the phosphate group of the peptide, and it interacts with the basic side chains and residues in the BC loop in an analogous manner. These residues and the phosphate group are further stabilized by interactions with a neighboring molecule in the crystal, which serves to close off the active site. Although the second molecule (MolB) does not have such crystal interactions and does not have a phosphate ion localized at the phosphotyrosine site, it too resembles the high affinity complex. In addition, the hydrophobic binding pockets in MolA and MolB closely resemble the YEEI complex.

The range of structures seen in the uncomplexed form presumably reflect an increased flexibility at the two binding sites in the absence of peptides, and differing sets of crystal contacts help stabilize particular conformations at each site. This is consistent with the results obtained for Abl and p85 SH2 domains in solution, where the phosphate-binding BC loop and the region surrounding the hydrophobic binding site are relatively disordered. This is in contrast with the YEEI complex, where the details of the binding sites are preserved in all three molecules of the crystal. The uncomplexed structure illustrated using MolD (Figures 4 and 5) is the extreme of the range observed in the crystal, but is likely to be representative of the flexibility afforded at the binding sites.

Discussion

Sequence Specificities of Different SH2 Domains

The plasticity of proteins makes it difficult to make precise predictions about the three-dimensional conformations and binding properties of other SH2 domains, based solely on the structure of Src SH2. Nevertheless, the strong conservation of the general architectural features of the domain makes it possible to obtain a qualitative picture of the structural basis for sequence discrimination. We illustrate this by comparing Src SH2 and the N-terminal SH2 domain of the p85α subunit of PIK (p85-N), for which the sequence specifity of peptide binding and the uncomplexed solution structure are known (Booker et al., 1992; Fantl et al., 1992; Piccione et al., submitted; Songyang et al., 1993; Escobedo et al., 1991). Both SH2 domains have strong preferences for large hydrophobic residues at the +3 position. However, Src SH2 favors isoleucine, while p85-N shows a clear selection for methionine. p85-N differs from Src at the +1 and +2 positions by showing a strong preference for methionine at +1 and no preference at +2 (Songyang et al., 1993).

Although methionine and isoleucine are both hydrophobic residues, they differ in shape. At the +3 site in p85-N, Gly BG3 and Ile βE4 of Src are replaced by the bulkier side chains of leucine and phenylalanine, respectively (Booker et al., 1992). In addition, the conformation of the BG loop is distinctly different, owing to a 6-residue insertion (Figure 2, and see below), and Tyr BG6 of p85-N may interact at the +3 site (Booker et al., 1992). The crowding of hydrophobic residues in this pocket is likely to select for the linear side chain of methionine over the bulkier and more sterically hindered isoleucine.

In Src the preference for Glu at +1 probably arises from interactions with Lys βD3 (see Figure 3). This lysine is conserved in p85, and indeed p85-N binds glutamate at +1 (Felder et al., 1993; Songyang et al., 1993). However, other changes in the p85-N sequence suggest that the aliphatic atoms of Lys βD3 may form part of a hydrophobic pocket at the +1 site, which would explain the stronger selection for methionine over glutamate. Replacement of Tyr βD5 by isoleucine in p85-N is likely to open up a hydrophobic pocket lined by the carbon atoms of Lys βD3, Ile βD5 (Tyr in Src), and Leu βC6 (Val in Src). In addition, Leu BG9 (inserted in p85-N) may interact at the +1 site and further contribute to the hydrophobicity. Such an interaction between the BG loop and the peptide residue at +1 would be consistent with cross-linking studies (Williams and Shoelson, 1993). At the +2 site, the selection for glutamate in Src appears to arise from the solvent-exposed nature of the site and the loose association with Arg βD′1. This residue is replaced by Phe in p85-N, which removes the negative selection against basic residues and may also help stabilize hyrophobic residues at the +2 site, leading to net lack of selectivity.

This kind of analysis can be extended to other SH2 domains. For example, the p85 C-terminal SH2 domain does not have as strong selection at +1. Ile βD5, which is part of the +1 hydrophobic pocket postulated for p85-N, is replaced by cysteine in p85-C, a polar residue. GAP SH2, which binds sequences with proline at +3 (Fantl et al., 1992), appears to have a more open hydrophobic pocket, owing to a shorter EF loop that contains two glycines. A particularly interesting variant is the Crk SH2 domain (data not shown), which has an 18-residue insertion at the D–D′ junction (Mayer et al., 1988; Overduin et al., 1992a). Such a large insertion in the middle of the peptide-binding surface is unique and can be expected to modulate the interactions with target peptides. Although speculative, these examples make clear that information now in hand for peptide binding to SH2 domains makes strong interplay possible between further peptide selection and protein mutagenesis experiments and structural modeling, which should lead rapidly to a comprehensive understanding of sequence specificity.

Conformational Changes Induced by Specific Binding

While the function of SH2 domains certainly involves the recruitment of SH2-containing proteins to form complexes at tyrosine phosphorylation sites, it has also been speculated that conformational changes in the SH2 domain upon phosphotyrosine binding may modulate enzyme activity (Pawson and Gish, 1992). This paper describes changes in three-dimensional structure that result from specific ligation of an SH2 domain and demonstrates that for Src these are relatively small and are localized to the immediate vicinity of the phosphotyrosine- and isoleucine-binding sites. The changes observed in Src are manifestations of increased structural flexibility in the absence of peptide and do not appear to be conformational triggers for the transmission of allosteric effects. In contrast, spectroscopic evidence suggests that the p85 SH2 domain undergoes a large conformational change upon ligation of specific peptides, possibly linked to allosteric stimulation of enzymatic activity (Panayotou et al., 1992; Shoelson et al., 1993). One source of a larger conformational change in p85 could be the BG loop, which is longer in p85 SH2 and could clamp down on bound peptides (Booker et al., 1992; Shoelson et al., 1993). However, the Src results demonstrate clearly that extensive conformational changes are not likely to be a general feature of SH2–peptide interactions.

General Implications for SH2 Function

A single SH2 domain is too small to carry out sequence-specific recognition by engulfing the peptide in a groove or intersubunit channel, as occurs with other well-characterized peptide–protein interactions. Instead, high affinity and specificity is achieved by an interaction that resembles the insertion of a two-pronged plug (the peptide) into a two-holed socket (the SH2 domain). This is in general agreement with results obtained independently by Eck et al. (submitted), who have determined the structure of the Lck SH2 domain complexed with the same YEEI peptide. In both Src and Lck, the phosphotyrosine and isoleucine (+3) interaction sites are on the edges of the SH2 domain, which limits flanking residues from engaging in specific interactions with SH2 domains. Thus, a necessary consequence of this plug-in-socket interaction is that the interface between the SH2 domain and the peptide is restricted

Table 1. X-Ray Data Collection Statistics

Derivatives	Resolution (Å)	Reflections	Unique	% Complete	R_{sym}[a]
Native uncomplexed	20.00–2.46	52,494	19,669	89.7	0.068
Derivatives					
Mercuric chloride	20.00–2.58	45,351	16,376	88.9	0.085
Irridium chloride	20.00–2.58	51,319	16,465	89.4	0.061
YEEI complex	20.00–2.7	19,885	11,714	89.1	0.067

Refinement Statistics

	Uncomplexed	YEEI Complex
Resolution	20.0–2.5 Å	20.0–2.7 Å
Reflections ($I > 2\sigma$)	19,219	11,420
Number of atoms	3,475	2,748
Solvent molecules	133	41
Crystallographic R factor		
Resolution 6.0–2.5 Å	0.185	
Resolution 6.0–2.7 Å		0.177
RMS deviation in bond lengths	0.012 Å	0.012 Å
RMS deviation in bond angles	2.9°	3.2°

[a] R_{sym}: agreement factor between intensities of symmetry-related reflections.

to a small region, not exceeding 5 to 6 residues. Proteins that contain multiple SH2 domains may exploit this compact binding interface by simultaneous recognition of more than one closely spaced phosphorylation site on target proteins. Alternatively, receptors or other SH2 targets that contain multiple binding sites may serve to tether different SH2-containing molecules in close proximity.

Although short peptide sequences are clearly the key elements in the interactions between SH2 domains and activated receptors, we have very little information on whether the binding affinity of phosphotyrosines in nonoptimal local sequence contexts can be enhanced by tertiary structural interactions. Particularly intriguing is the nature of the structural interactions, if any, between SH2 and SH3 domains, which are smaller modules that bind unmodified peptide sequences (Koch et al., 1991; Cicchetti et al., 1992). That such interactions may exist is suggested by the fact that they usually occur together in enzymes as well as in "adaptor" proteins that do not contain catalytic domains (Koch et al., 1991; Mayer and Baltimore, 1993). The availability of three-dimensional structural information for SH2 and SH3 domains and the identification of their peptide-binding surfaces (Musacchio et al., 1992; Yu et al., 1992) now makes possible the design of decisive experiments aimed at deciphering the roles played by these modules in the much larger intact proteins of which they are a part.

Experimental Procedures

Crystallization

The SH2 domain of v-Src was overexpressed in Escherichia coli and purified as described (Waksman et al., 1992). The purified protein was concentrated to 250 mg/ml (20 mM) by ultrafiltration in a buffer containing 10 mM HEPES (pH 8.0), 5 mM EDTA, and 5 mM dithiothreitol. Crystallization conditions were scanned using the hanging drop method (McPherson, 1990). In the absence of phosphate ions and peptide, large hexagonal crystals were obtained with polyethylene glycol (average M_r = 4000) as the precipitant. The crystals show diffraction spots to 2 Å spacings, but the diffraction pattern is streaked along certain directions and the crystals are not useable for structure determination. Addition of 200 mM K_2HPO_4 to the crystallization conditions results in the appearance of small rounded plate-like crystals. Large crystals suitable for data collection were obtained by repeated seeding. Diffraction patterns obtained with these crystals of the uncomplexed form show no evidence of disorder. The crystals of the uncomplexed form are orthorhombic ($P2_12_12$; a = 110.9 Å, b = 86.2 Å, c = 58.9 Å), with four molecules in the asymmetric unit and an approximate solvent content of 58%.

The YEEI phosphopeptide was synthesized, purified, and characterized as described (Domchek et al., 1992). All attempts to soak peptides into crystals grown in the absence of peptide resulted in cracking and the loss of diffraction. Cocrystals of the high affinity peptide–SH2 complex were obtained by scanning a varied set of conditions using equimolar (10 mM) concentrations of peptide and protein. One large single crystal of the complex (0.5 × 0.5 × 0.3 mm^3) was obtained within 2 weeks from a drop containing the protein–peptide mixture in 10 mM HEPES buffer at pH 8.0, 5 mM EDTA, 5 mM dithiothreitol, and 10% polyethylene glycol (average M_r = 4000), equilibrated against a reservoir containing 30% 2-methyl-2,4-pentanediol. This large crystal sufficed for data collection to 2.7 Å (see below), but proved to be irreproducible. Similar conditions yielded small needle-like crystals, and seeding experiments are required to grow large crystals. The crystal used for data collection is tetragonal ($P4_1$; a = b = 93.3 Å, c = 55.0 Å) with three molecules in the asymmetric unit and an approximate solvent content of 60%.

X-Ray Data Collection

Earlier attempts at SH2 structure determination by multiple isomorphous replacement (MIR) were focused on crystals of the uncomplexed form, but severe nonisomorphism in derivative crystals led to uninterpretable electron density maps. These derivatives proved to be useful in structure determination by molecular replacement, subsequent to the determination of the structure of the low affinity complex by MIR (Waksman et al., 1992). Three data sets were used in the analysis of the uncomplexed form: a native data set and two derivative data sets (mercuric chloride and iridium chloride), all to 2.5 Å. The derivative crystals (but not the native) were cross-linked with glutaraldehyde, as described previously (Waksman et al., 1992). A single crystal was used to collect data to 2.7 Å for the high affinity complex. The diffraction pattern extended to beyond 2.5 Å initially, but decayed during the course of data collection. All X-ray analysis was carried out at room temperature.

X-ray intensities were measured by the oscillation method, using a Rigaku R-AXIS IIC imaging phosphor area detector, mounted on a Rigaku RU200 rotating anode X-ray generator (Molecular Structure Corporation, Houston, Texas). For uncomplexed SH2, crystal to detector distances and exposure times were 130 mm and 20 min, respectively, for 2.2° oscillations. For the high affinity complex, crystal to detector distances and exposure times were 130 mm and 25 min, respectively, for 2.0° oscillations. Data processing and reduction were done using software provided by Rigaku and the programs DENZO and

SCALEPACK (Z. Otwinowski, unpublished data). X-ray data collection statistics are reported in Table 1.

Structure Determination of the Uncomplexed Form

Structure determination was carried out by the molecular replacement method (Rossmann, 1972; Brünger, 1990) using the program X-PLOR (Brünger, 1988). Rotation search in Patterson space was carried out using the model originating from the peptide A–SH2 complex structure from which the peptide was deleted (Waksman et al., 1992). The highest peaks of the cross rotation function were then refined using Patterson correlation refinement (Brünger, 1990). The molecule was oriented according to the highest resulting peak, and a three-dimensional translation search was carried out, resulting in a peak at 7.4 σ above the mean and corresponding to the position of a molecule labeled MolA. A self-rotation function revealed two peaks corresponding to 2-fold rotations. One of these ($\psi = 60°$, $\phi = 0°$, and $\kappa = 180°$) was applied to MolA, followed by a three-dimensional search. The highest peak of the translation function was at 11.8 σ and corresponds to a second molecule labeled MolB. Determination of the orientation and positions of the two remaining molecules proved to be difficult, and a combination of MIR and molecular replacement was used to locate them. Heavy atom derivatives were obtained by soaking glutaraldehyde cross-linked crystals with 100 mM iridium chloride or 1 mM mercuric chloride (Table 1). Phases calculated using MIR methods alone yielded very noisy electron density maps with no recognizable features and were not pursued further. Instead, the partial atomic model resulting from the location of the first two molecules was used to calculate protein phases. Heavy atom difference Fourier maps were then calculated using these protein phases and the measured differences in native and derivative intensities. Peaks in these maps, corresponding to the positions of mercury and iridium chloride ions, immediately confirmed the correctness of the partial solution. The negatively charged iridium hexachloride ions were seen to be bound at the phosphotyrosine site, and peaks corresponding to mercury atoms were found in the vicinity of cysteines. Two additional sets of iridium and mercury peaks were found that corresponded to the locations of the two missing molecules (labeled MolC and MolD). These were placed by searching through the rotation function list and finding orientations and translations that were consistent with the observed heavy metal positions. Refinement of the structure included several cycles of simulated annealing refinement using X-PLOR (Weis et al., 1990), in order to remove bias toward the starting model, followed by manual inspection of electron density maps and rebuilding of the model using the program O (Jones et al., 1991). The net charge on all side chains was set to 0. The final model has an R factor of 18.5% (6.0–2.5 Å), with excellent stereochemistry (the RMS deviation from ideal geometry is 0.012 Å for bond lengths and 2.9° for bond angles; see Table 1).

Structure Determination of the High Affinity Complex

Structure determination proceeded as for the uncomplexed form, except that MIR data were not used. The SH2–peptide B complex of Waksman et al. (1992) was used as the search model, with the peptide deleted. The two highest peaks of the rotation function gave the orientation of two molecules (labeled Mol1 and Mol2). Consecutive translation searches resulted in peaks at 8.1 σ and 10.6 σ, respectively. The third molecule was found by searching through the rotation function list (obtained by Patterson correlation refinement) and carrying out three-dimensional searches on each rotation, keeping the positions of the first two molecules fixed. The tenth highest unique peak in the rotation list yielded a molecular position (Mol3) that was consistent with crystal packing. The correctness of the solution was immediately apparent, as density for the phosphotyrosine and the rest of the peptide was clearly visible in difference Fourier maps in all three molecules.

After building independent models for the peptide in all three molecules, a solvent mask was calculated and used in further refinement (Weis et al., 1990). As before, simulated annealing refinement (Weis et al., 1990) was carried out, followed by manual inspection and rebuilding. The correctness of the final model was checked using simulated annealing omit maps (Hodel et al., 1992). The model presented here contains peptide residues −3 to +5 in Mol1, −3 to +3 in Mol2, and −2 to +7 in Mol3. Alanine residues were built in positions where density for side chain was very poor, as is the case for position −3 in Mol1 and position −1 for Mol3. The R factor is 17.7%, including data from 6.0 Å to 2.7 Å. The model includes 41 solvent molecules interpreted as water. The RMS deviation for ideal geometry is 0.012 Å for bond lengths and 3.2° for bond angles (Table 1). One manifestation of differences between crystal packing interactions for the three molecules is that Mol3 exhibits significantly higher motion or disorder, as judged by the relative values of the crystallographic temperature factors. The average temperature factor for all atoms in helices and strands for Mol1 and Mol2 is 24 Å^2 and 30 Å^2, respectively, whereas it is 47 Å^2 for Mol3. Despite the higher disorder in Mol3, electron density maps are quite clear for this molecule.

Examination of Ramachandran plots for both structures shows violations limited to the C-terminal and the N-terminal residues of the different molecules in the asymmetric units. Density is uninterrupted and well defined for the structure of the high affinity peptide–SH2 complex in all regions of the protein in all three molecules. For the uncomplexed SH2 structure the density of the phosphate-binding loop is poor and limited to the polypeptide backbone in all molecules except MolA, where it is well defined (a phosphate ion is bound at the phosphotyrosine site in MolA). Density is discontinuous in the CD loop in all four molecules.

Acknowledgments

We thank L. C. Cantley, M. Eck, and S. C. Harrison for sharing data and insights prior to publication, D. Baltimore, S. K. Burley, and H. Hanafusa for helpful discussions, G. A. Petsko for suggesting the combination of MIR and molecular replacement, and K. L. Clark and J. L. Kim for assistance with DENZO, which was kindly provided by Z. Otwinowski. We are grateful to G. D. Booker and I. D. Campbell for providing the p85 atomic coordinates. This work was supported in part by grants from the National Institutes of Health (D. C., J. K., and S. E. S.), the National Science Foundation (S. E. S.), and the Pew Foundation (J. K.).

Received January 25, 1993; revised February 5, 1993.

References

Backer, J. M., Myers, M. G., Shoelson, S. E., Chin, D. J., Sun, X.-J., Miralpeix, M., Hu, P., Margolis, B., Skolnik, E. Y., Schlessinger, J., and White, M. F. (1992). Phosphatidylinositol 3′-kinase is activated by association with IRS-1 during insulin stimulation. EMBO J, *11*, 3469–3479.

Birge, R. B., Fajardo, J. E., Mayer, B. J., and Hanafusa, H. (1992). Tyrosine-phosphorylated epidermal growth factor receptor and cellular p130 provide high affinity binding substrates to analyze crk-phosphotyrosine-dependent interactions in vitro. J. Biol. Chem. *267*, 10588–10595.

Booker, G. W., Breeze, A. L., Downing, A. K., Panayotou, G., Gout, I., Waterfield, M. D., and Campbell, I. D. (1992). Structure of an SH2 domain of the p85α subunit of phosphatidylinositol-3–OH kinase. Nature *358*, 684–687.

Brünger, A. T. (1988). X-PLOR (Version 2.2) Manual (New Haven: Yale University).

Brünger, A. T. (1990). Extension of molecular replacement: a new search strategy based on Patterson correlation refinement. Acta Crystallogr. *46*, 46–57.

Cantley, L. C., Auger, K. R., Carpenter, C., Duckworth, B., Graziani, A., Kapeller, R., and Soltoff, S. (1991). Oncogenes and signal transduction. Cell *64*, 281–302.

Cicchetti, P., Mayer, B. J., Theil, G., and Baltimore, D. (1992). Identification of a protein that binds to the SH3 region of abl and is similar to Bcr and GAP-rho. Science *257*, 803–806.

Domchek, S. M., Auger, K. R., Chatterjee, S., Burke, T. R., and Shoelson, S. E. (1992). Inhibition of SH2 domain/phosphoprotein association by a nonhydrolyzable phosphonopeptide. Biochemistry *31*, 9865–9870.

Escobedo, J. A., Kaplan, D. R., Kavanaugh, W. M., Turck, C. W., and Williams, L. T. (1991). A phosphatidylinositol 3-kinase binds to platelet-derived growth factor receptors through a specific receptor sequence containing phosphotyrosine. Mol. Cell. Biol, *11*, 1125–1132.

Fantl, W. J., Escobedo, J. A., Martin, G. A., Turck, C. W., del Rosario, M., McCormick, F., and Williams, L. T. (1992). Distinct phosphotyrosines on a growth factor receptor bind to specific molecules that mediate different signaling pathways. Cell *69*, 413–423.

Felder, S., Zhou, M., Hu, P., Urena, J., Ullrich, A., Chaudhury, M.,

White, M., Shoelson, S., and Schlessinger, J. (1993). The binding of SH2 domains to tyrosine phosphorylated peptides exhibits high affinity binding yet rapid dissociation and exchange. Mol. Cell. Biol., in press.

Gilson, M. K., Sharp, K. A., and Honig, B. H. (1988). Calculating the electrostatic potential of molecules in solution: method and error assessment. J. Comp. Chem. *9*, 327–335.

Hodel, A., Kim, S.-H., and Brünger, A. T. (1992). Model bias in macromolecular structures. Acta Crystallogr. *48*, 851–858.

Janin, J., and Chothia, C. (1990). The structure of protein-protein recognition sites. J. Biol. Chem. *265*, 16027–16030.

Jones, T. A., Zou, J. Y., Cowan, S. W., and Kjeldgaard, M. (1991). Improved methods for building protein models in electron density maps and the location of errors in these models. Acta Crystallogr. *47*, 110–119.

Kashishian, A., Kazlauskas, A., and Cooper, J. A. (1992). Phosphorylation sites in the PDGF receptor with different specificities for binding GAP and PI3 kinase in vivo. EMBO J. *11*, 1373–1381.

Klippel, A., Escobedo, J. A., Fantl, W. J., and Williams, L. T. (1992). The C-terminal SH2 domain of p85 accounts for the high affinity and specificity of the binding of phosphatidylinositol 3-kinase to phosphorylated platelet-derived growth factor β receptor. Mol. Cell. Biol. *12*, 1451–1459.

Koch, C. A., Anderson, D., Moran, M. F., Ellis, C., and Pawson, T. (1991). SH2 and SH3 domains: elements that control interactions of cytoplasmic signaling proteins. Science *252*, 668–674.

Liu, X., Brodeur, S. R., Gish, G., Songyang, Z., Cantley, L. C., Laudano, A. P., and Pawson, T. (1993). Regulation of c-src tyrosine kinase activity by the src SH2 domain. Oncogene, in press.

Mayer, B. J., and Baltimore, D. (1993). Signalling through SH2 and SH3 domains. Trends Cell Biol. *3*, 8–13.

Mayer, B. J., Hamaguchi, M., and Hanafusa, H. (1988). A novel viral oncogene with structural similarity to phospholipase C. Nature *332*, 272–275.

McPherson, A. (1990). Current approaches to macromolecular crystallization. Eur. J. Biochem. *189*, 1–23.

Moran, M. F., Koch, C. A., Anderson, D., Ellis, C., England, L., Martin, G. S., and Pawson, T. (1990). Src homology region 2 domains direct protein–protein interactions in signal transduction. Proc. Natl. Acad. Sci. USA *87*, 8622–8626.

Musacchio, A., Noble, M., Pauptit, R., Wierenga, R., and Saraste, M. (1992). Crystal structure of a Src-homology 3 (SH3) domain. Nature *359*, 851–855.

Nicholls, A., Sharp, K. A., and Honig, B. (1991). Protein folding and association: insights from the interfacial and thermodynamic properties of hydrocarbons. Protein Struct. Funct. Genet *11*, 281–296.

O'Brien, M. C., Fukui, Y., and Hanafusa, H. (1990). Activation of proto-oncogene p60c-src by point mutations in the SH2 domain. Mol. Cell. Biol. *10*, 2855–2862.

Overduin, M., Mayer, B., Rios, C. B., Baltimore, D., and Cowburn, D. (1992a). Secondary structure of Src homology 2 domain of c-abl by heteronuclear NMR spectroscopy in solution. Proc. Natl. Acad. Sci. USA *89*, 11673–11677.

Overduin, M., Rios, C. B., Mayer, B. J., Baltimore, D., and Cowburn, D. (1992b). Three-dimensional solution structure of the src homology 2 domain of c-abl. Cell *70*, 697–704.

Panayotou, G., Bax, B., Gout, I., Federwisch, M., Wrobiowski, B., Dhand, R., Fry, M. J., Blundell, T. L., Wolimer, A., and Waterfield, M. D. (1992). Interaction of the p85 subunit of PI 3-kinase and its N-terminal SH2 domain with a PDGF receptor phosphorylation site: structural features and analysis of conformational changes. EMBO J. *11*, 4261–4272.

Pawson, T., and Gish, G. D. (1992). SH2 and SH3 domains: from structure to function. Cell *71*, 359–362.

Richards, F. M. (1977). Areas, volumes, packing and protein structure. Annu. Rev. Biophys. Bioeng. *6*, 151–176.

Rossmann, M. G. (1972). The molecular replacement method. In the International Scientific Review Series, Number 13 (New York: Gordon and Breach).

Rotin, D., Margolis, B., Mohammadi, M., Daly, R. J., Dawn, G., Li, N., Fischer, E. H., Burgess, W. H., Ullrich, A., and Schlessinger, J. (1992). SH2 domains prevent tyrosine dephosphorylation of the EGF receptor; identification of Tyr 992 as the high affinity binding site for SH2 domains of phospholipase Cγ. EMBO J. *11*, 559–567.

Roussel, R. R., Brodeur, S. R., Shalloway, D., and Laudano, A. P. (1991). Selective binding of activated pp60 c-src by an immobilized synthetic phosphopeptide modeled on the carboxyl terminus of pp60 c-src. Proc. Natl. Acad. Sci. USA *88*, 10696–10700.

Sadowski, I., Stone, J. C., and Pawson, T. (1986). A noncatalytic domain conserved among cytoplasmic protein-tyrosine kinases modifies the kinase function and transforming activity of fujinami sarcoma virus $p130^{gag\text{-}fps}$, Mol. Cell. Biol. *6*, 4396–4408.

Shoelson, S. E., Sivaraj, M., Williams, K. P., Hu, P., Schlessinger, J., and Weiss, M. A. (1993). Specific phosphopeptide binding regulates a conformational change in the PI 3-kinase SH2 domain associated with enzyme activation. EMBO J., in press.

Songyang, Z., Shoelson, S. E., Chaudhuri, M., Gish, G., Pawson, T., Haser, W. G., King, F., Roberts, T., Ratnofsky, S., Lechleider, R. J., Neel, B. G., Birge, R. B., Fajardo, J. E., Chou, M. M., Hanafusa, H., Schaffhausen, B., and Cantley, L. C. (1993). SH2 domains recognize specific phosphopeptide sequences. Cell *72*, this issue.

Waksman, G., Kominos, D., Robertson, S. R., Pant, N., Baltimore, D., Birge, R. B., Cowburn, D., Hanafusa, H., Mayer, B. J., Overduin, M., Resh, M. D., Rios, C. B., Silverman, L., and Kuriyan, J. (1992). Crystal structure of the phosphotyrosine recognition domain SH2 of v-src complexed with tyrosine-phosphorylated peptides. Nature *358*, 646–653.

Weis, W. I., Brünger, A. T., Skehel, J. J., and Wiley, D. C. (1990). Refinement of the Influenza virus hemagglutinin by simulated annealing. J. Mol. Biol. *212*, 737–761.

Williams, K. P., and Shoelson, S. E. (1993). A photaffinity scan maps regions of the p85 SH2 domain involved in phosphoprotein binding. J. Biol. Chem., in press.

Yu, H., Rosen, M. K., Shin, T. B., Seidel-Duggan, C., Brugge, J. S., and Schreiber, S. L. (1992). Solution structure of the SH3 domain of Src and identification of its ligand-binding site. Science *258*, 1665–1668.

Note Added in Proof

The papers referred to throughout as Eck et al., Payne et al., and Piccione et al., submitted, are now in press: Eck, M., Shoelson, S. E., and Harrison, S. C. (1993). Recognition of a high affinity phosphotyrosyl peptide by the Src homology 2 domain of $p56^{lck}$. Payne, G., Shoelson, S. E., Gish, G., Pawson, T., and Walsh, C. T. (1993). Binding kinetics of Lck and Src SH2 domain/phosphopeptide interactions by competitiion assay and surface plasmon resonance. Proc. Natl. Acad. Sci. USA. Piccione, E., Case, R. D., Domchek, S. M., Hu, P., Chaudhuri, M., Backer, J. M., Schlessinger, J., and Schoelson, S. E. (1993). PI 3-kinase p85 SH2 domain specificity defined by direct phosphopeptide/SH2 domain binding. Biochemistry.